

Molecular Characterization of Water Rattan Palm (*Calamus angustifolius* Griff.) from Kampar River, Riau Province, Indonesia Using *matK* and *trnL-trnL-trnF* Intergenic Spacer

Hapiz Al Khairi^{1,2}, Dewi Indriyani Roslim^{1,*}, Aristyanti Devie Vitovang¹, Meisita Hariani¹, Herman¹, Wahyu Lestari¹, Adiwirman³, Aldy Riau Wansyah Hasibuan^{1,2}, Linda Novita⁴, Siti Zulaeha⁴, Irni Furnawanthi Hindaningrum⁴

¹ Department of Biology, Faculty of Mathematics and Natural Sciences, University of Riau, Binawidya Campus, Jl HR Soebrantas Km 12.5, Panam, Pekanbaru, Riau, Indonesia; ² Department of Tropical Biology, Faculty of Biology, Universitas Gadjah Mada. Jl. Teknik Selatan, Sinduadi. Mlati, Sleman, 55281. Special Region of Yogyakarta, Indonesia; ³ Department of Agrotechnology, Faculty of Agriculture, University of Riau, Binawidya Campus, Jl HR Soebrantas Km 12.5, Panam, Pekanbaru, Riau, 28293, Indonesia; ⁴ Research Center for Applied Botany, National Research and Innovation Agency, Jl. Raya Jakarta-Bogor Km. 46, Cibinong, Bogor, Jawa Barat, 16911, Indonesia

Received: August 24, 2024; Revised: October 10, 2024; Accepted: October 22, 2024

Abstract

Calamus angustifolius Griff., commonly known as water rattan, is an important species found in the Kampar River region of Riau Province, Indonesia. This rattan is a valuable non-timber forest product (NTFP) playing a crucial role in rural economies, especially in Indonesia, which supplies about 80% of the global rattan market. This species thrives in watery habitats such as peat swamps and floodplain rivers, contributing to the structural complexity of tropical forests and supporting diverse wildlife. Understanding its molecular characterization and morphological analysis is crucial for its conservation and sustainable utilization. This study employed *matK* and *trnL-trnL-trnF* intergenic spacer DNA markers for molecular characterization. DNA sequences were analyzed using MEGA11. In this study, the obtained *matK* and *trnL-trnL-trnF* IGS sequences showed lengths 848 bp and 867 bp, respectively. There was no critical nucleotide based on *trnL-trnL-trnF* IGS, but three critical nucleotides were found based on *matK*. The study found significant genetic variation within the *matK* region, with unique nucleotide positions specific to *C. angustifolius*. However, the *trnL-trnF* region showed less variability, limiting its utility for species differentiation. The high frequency of A+T nucleotides in both markers indicates specific evolutionary patterns in this genus. This rattan is closely similar to *C. aruensis* and *Pigafetta elata* genetically. The *matK* gene proved to be a reliable DNA barcode, providing clear and distinct genetic profiles essential for species identification and genetic mapping. In contrast, the *trnL-trnL-trnF* IGS showed limited utility as a DNA barcode due to its low variability and poor resolution in distinguishing between individuals. This research underscores the need for genetic resource conservation to prevent the loss of valuable germplasm. These findings provide a foundation for conservation efforts and sustainable resource management of water rattan.

Keywords: *Calamus angustifolius*, water rattan, *matK*, *trnL-trnL-trnF* intergenic spacer, DNA barcode, molecular characterization, Riau, Indonesia.

1. Introduction

Due to high morphological similarities among species, the taxonomy of the rattan genus *Calamus* presents challenges for accurate species identification, often leading to ambiguity in classification. According to all available phylogenetic data, the rattan genus *Calamus* is the largest of all palm (Arecaceae) genera and is nested inside the subtribe Calaminae (Calameae: Calamoideae). *Ceratolobus*, *Daemonorops*, *Pogonotium*, and *Retispatha* are the other four genera in the subtribe (Baker, 2015). Recent studies have highlighted the challenges in identifying species within the genus *Calamus* due to the complexity of morphological characteristics. One notable

approach to overcome these challenges is the use of DNA barcoding (Kurian *et al.*, 2020). The furniture business is the main application for rattan, a vine that grows in tropical woods (Myers, 2015). The role that non-timber forest products (NTFPs) play in rural communities' development, livelihoods, and efforts to reduce poverty has garnered increased attention in the last few decades (Suleiman *et al.*, 2017). Similarly, *Calamus angustifolius* as one of the NTFPs is also utilized as a raw material in various industries.

Calamus angustifolius is a valuable source of rattan, which is used in the production of furniture, handicrafts, and other products. The rattan industry supports livelihoods in rural communities and contributes to local and national economies (Siebert, 2005). This plant also

* Corresponding author. e-mail: dewiindriyaniroslim@gmail.com.

contributes to the structural complexity of tropical forests, providing habitat and support for various organisms, including birds, insects, and other plants. Its climbing nature helps create vertical habitat layers, which are crucial for species that depend on understory and canopy environments.

The habitat of *C. angustifolius* consists of watery areas, such as peat swamps, river basins, and floodplain rivers in Indonesia. Numerous floodplain ecosystems in the province of Riau are home to genetically diverse endemic plants and animals (Roslim *et al.*, 2016) including habitat for *C. angustifolius*. This rattan grows in clumps and climbs on other plants. Uniquely, this type of rattan can be consumed because of its sweet taste and is also commonly referred to as "rotan getah manis." The shoot (umbut) of the young plant is often used by the Malay community in Riau to make a food preparation called "pangkek" (Ayu, 2018).

As the largest rattan-producing country, Indonesia has contributed approximately 80% of the world's rattan needs. There are several key points in presenting rattan as a commodity used in society, namely identifying its types and origins (Kaliky, 2018). Rattan has a very variable form, making it difficult to identify different species. Flowers and fruits serve as the morphological characters used for identification, but obtaining flowers from these plants is very difficult. Similarly, the similarity of fruits between species is strikingly close, making identification a time-consuming and challenging process.

One of the finest ways to research molecular taxonomy and identify and distinguish between species is through molecular analysis (Al-Rawashdeh, 2011). The shortcomings of morphological features may be overcome and species identification may be sped up with the use of DNA barcoding technique (Amandita *et al.*, 2019). These techniques have proven highly effective with biochemical and morphological indicators for species identification and biodiversity assessment. This helps in the formulation of effective conservation strategies and the monitoring of endangered species (Antil *et al.*, 2023; Mir *et al.*, 2021; Odah, 2023). Unfortunately, there is no nucleotide-based validation of *C. angustifolius* in Genbank.

When it came to distinguishing between species, the varied combinations of the two loci were more effective than either locus individually (Ho *et al.*, 2021). To generate DNA barcodes in plant systematics, cpDNA barcode sequences are suitable for application. Commonly used genes are *rbcL*, *matK*, *rpoB*, *rpoCI*, *ycf5(ccsA)*, *trnH-psbA*, *trnL-F* (Chac and Thinh, 2023). On the other hand, the popular loci are *rbcL*, the *trnL-F intergenic spacer*, *matK*, *ndhF* and *atpB* (Awomukwu *et al.*, 2015). The two DNA barcodes with the most variance, *matK* and *trnL-trnF IGS*, are thought to be able to identify plants into species and subspecies levels (Herman *et al.*, 2023; Tanaka

and Ito, 2020). In addition, the benefits of modern molecular markers like SNPs or *ITS* for future studies could point toward future research directions (Baldwin *et al.*, 1995; Davey and Blaxter, 2010).

The *matK* gene encodes the maturaseK protein found in plant chloroplasts and has a length of approximately 1,500 base pairs in angiosperms (Kar and Goyal, 2015). It is located within the intron of the *trnK* gene. The *matK* gene functions in maturation, specifically splicing type II introns from RNA transcripts (Mustafa *et al.*, 2018). Unlike *matK*, which encodes a protein, the *trnL-trnF IGS* is only a region covering the intron of the *trnL* gene and the spacer between the *trnL* and *trnF* genes and does not encode a functional gene (Borsch and Quandt, 2009; Shaw *et al.*, 2007).

The CBOL plant working group proposed the use of *rbcL* and *matK* as a "core" universal plant barcoding regions (CBOL Plant Working Group, 2009). It is known that *matK* is more commonly used in molecular identification compared to the *rbcL* gene (Roslim, 2017). The proof of the usefulness of *matK* primer is when they are used in certain species or taxa (Amandita *et al.*, 2019). There are already traces of proof of the success of using *matK* in solving taxonomic problems in palms or the Arecaceae family (Yao *et al.*, 2023), but not yet in the *C. angustifolius* species. The formation of genetic collections is necessary for the conservation of genetic resources to prevent genetic erosion, resulting in the loss of valuable germplasm. Here, in this study, we described the molecular characteristics of water rattan palm (*Calamus angustifolius* Griff.) determined by *matK* and *trnL-trnL-trnF intergenic spacer*.

2. Materials and Methods

2.1. Material and procedure

Plant materials, water rattan palms, used in this study were collected and identified from three different locations in Riau Province. First, from Teratak Buluh Village (3 individuals, with 0°23'24.6"N 101°25'57.5"E coordinate of location), secondly from Langgam Village, Pelalawan (1 individual, with 0°16'27.2"N 101°42'30.0"E coordinate of location), and lastly from Kualu Village, Kubang (2 individuals, with 0°23'21.7"N 101°20'44.3"E coordinate of location) (Figure 1). DNA was extracted from the young leaf sample cut into small pieces and crushed by adding liquid nitrogen to the mortar, then the extraction process was carried out using the Genomic DNA Mini Kit Plant (Geneaid, New Taipei City, Taiwan) according to the manufacturer's protocol. The extracted DNA was visualized and qualified by using electrophoresis (Mupid-exU), and it was stored at -20°C.

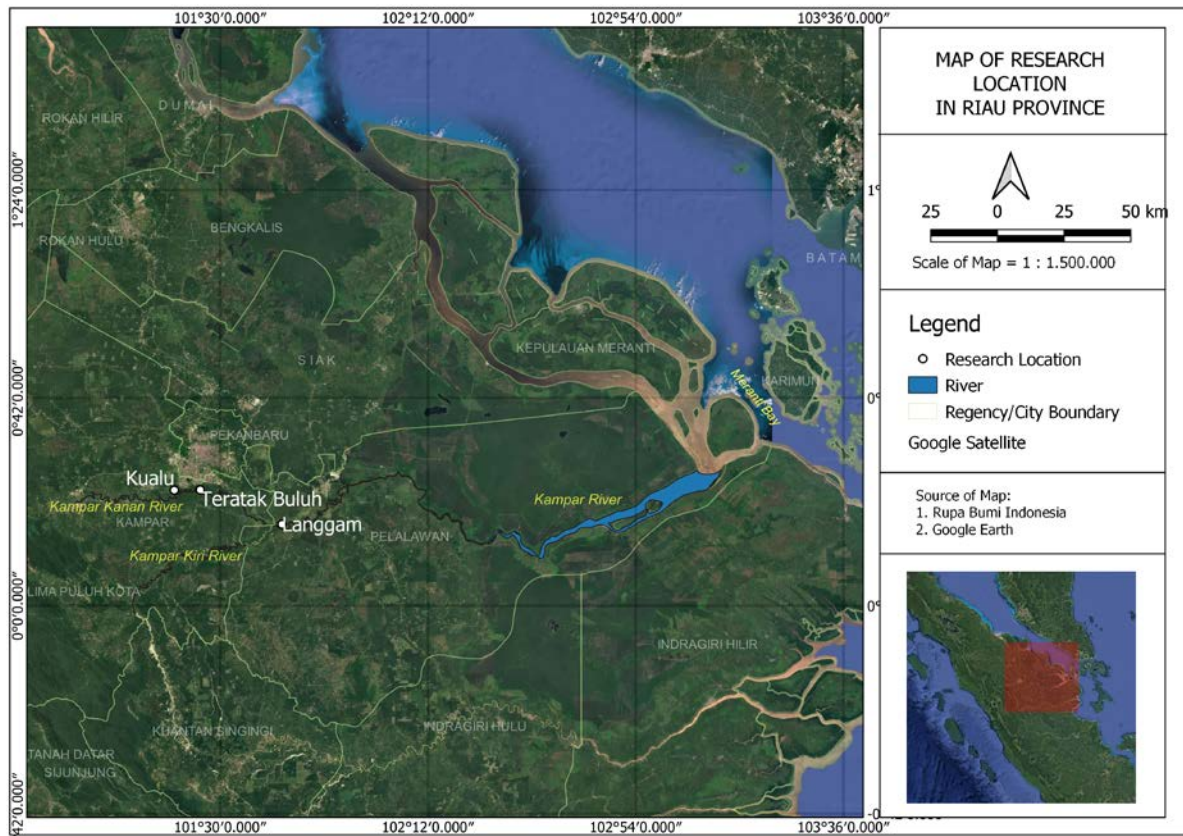


Figure 1. The map of water rattan palm sample used in this study (elaborated in Google Earth 2024).

Polymerase Chain Reaction (PCR) amplification was carried out in a total volume of 50 μ l, containing final reaction compositions as follows: 1X PCR buffer, 0.2 mM dNTPs, 2.4 μ M for each primer, and 2 U/ μ L DreamTaq DNA polymerase (*Thermo Scientific*). Two primer pairs were used for PCR amplification, matK-413f-1: 5'-TAA TTT ACR ATC AAT TCA TTC AAT ATT TCC-3' and matK-1227r-3: 5'-GAR GAT CCR CTR TRA TAA TGA AAA AGA TTT -3' for amplifying the *matK* region (Heckenhauer *et al.*, 2016) and B49317_F2: 5'-CGA AAT CGG TAG ACG CTA CG-3' and A50272_R3: 5'-ATT TGA ACT GGT GAC ACG AG-3' for amplifying the *trnL-trnL-trnF IGS* (Taberlet *et al.*, 1991).

The conditions for PCR amplification were as follows: 3 min at 95 °C, 35 cycles of 95 °C (45 s) denature, 49.2 °C for *trnL-trnLtrnF IGS* and 47.5 °C for *matK* (45 s) annealing, and 72 °C (90 s) extension, with a final extension cycle of 72 °C for 10 min (Herman *et al.*, 2023). Amplicon of PCR was separated by electrophoresis in a 1% agarose gel added with 3 μ l ethidium bromide, for 45 minutes at 50 Volts in 1x Tris-Borate-EDTA (TBE). The amplified products were resolved in 1% agarose gel using 1X TBE buffer, and then the PCR products were sequenced to PT. Genetika Science Indonesia as an intermediary, for further sequencing to be carried out at First Base Laboratories, Malaysia.

2.2. Data analysis

DNA sequence data analysis followed the procedure developed by Herman *et al.* (2023). DNA sequences forward and reverse primers were then aligned by using the BioEdit version 7.0.0 program (Hall, 1999). The BLASTn program on the <https://blast.ncbi.nlm.nih.gov/> site was then used for both *matK* and *trnL-trnL-trnF IGS*

to determine the similarity of the sequences studied to those in the GenBank database. Besides, the BOLD on the <https://v3.boldsystems.org/> program is also used as an addition to similar sequence checks, specifically for *matK*. The top 10-12 accessions were used to determine nucleotide variations between the studied accessions. Management and analyzed DNA sequences were performed with MESQUITE (Maddison and Maddison, 2023). Multiple alignments were done using ClustalW (Thompson *et al.*, 1994). Phylogenetic analysis were done by using the MEGA 11 (Tamura *et al.*, 2021) using the different methods to perform three different phylogenetic trees, such as maximum likelihood (ML), neighbor joining (NJ), and maximum parsimony (MP). The trees were evaluated using methods like the bootstrap re-sampling method with 1000 replicates (Felsenstein, 1985) to assess its accuracy, assuring that the branches that frequently emerge are most likely to reflect the true evolutionary relationship.

3. Results

3.1. Species taxonomic description

Morphological features of Water Rattan Palm (*C. angustifolius*) are illustrated in Figure 2. Characteristic of this plant's morphology is habitating bushes, growing clusters, and climbing on other plants (Figure 2a). This rattan has a splintered, brown-green stem with a slightly rough stem surface (Figure 2b). The edible part of the stem is illustrated in Figure 2d. The leaves are green with a subulate leaf shape, the leaf ends are acuminate with a flat leaf edge (entire) and the leaves are placed in pairs and sitting leaves face to face. The top and bottom surfaces of

the leaves tend to have the same color, but on the bottom surface, some thorns are not so sharp. The rodent is round and has scratches on the skin of the fruit. When it is divided straight, it appears that there is an orange broth (Figure 2c). The old rod has a brown-colored thorn with a

diameter of 20-25 mm and a street length of 30-35 cm, but it is arranged irregularly (Figure 2e). The fruit is green when it is young and will be yellowish when it is ripe. This rattan is also edible and has a delicate, clay flavor.



Figure 2. The morphology of rotan getah manis or water rattan palm (*Calamus angustifolius* Griff.) from Teratak Buluh, Kampar District, Riau Province, Indonesia. (a) Habitats, (b) fruit in bunches, (c) a fruit (upper) and a fruit sliced crosswise (lower), (d) edible rattan shoot, and (e) spiny stem. The red circle shows an edible rattan shoot.

3.2. Phylogenetic analysis for the gene *matK*

Eleven sequences were obtained (Table 1) and submitted to the GenBank Nucleotide database. All of the *matK* gene products size is about 848 bp of chloroplast plastid region for the *C. angustifolius* species, without any differences of nucleotides obtained. The sequence obtained was then searched into GenBank with BLASTn analysis (Table 2). The *matK* sequence of *C. angustifolius* has a 99% similarity with *C. jenkinsianus*, *C. tetradactylus*, *C. walkeri*, *C. henryanus*, *C. aruensis*, *C. castaneus*, and *C. caryotoides*, with the highest similarity score 99.53% for *C. jenkinsianus*. The sequence exhibited 98% similarity to *C. viminalis*, in addition to other plant species including *Pigafetta elata* and *Metroxylon warburgii*. The BOLD identification system also shows 99% similarity with *C. castaneus* and 98% with *C. viminalis* for plant species of *Calamus*.

Table 1. List of sequences obtained and submitted to Genbank from this study.

No	DNA Barcode	Sample Origin	Voucher	No. of Accession
1	<i>matK</i>	Teratak Buluh	DIR104	OQ174528
2			DIR105	OQ174529
3			DIR106	OQ174530
4		Langgam	DIR124	OQ942619
5	<i>trnL-trnL-trnF IGS</i>	Teratak Buluh	DIR113	OQ174515
6			DIR114	OQ174516
7			DIR115	OQ174517
8		Kualu	DIR122	OQ325046
9			DIR123	OQ325047
10		Langgam	DIR125	OQ942620
11			DIR031	MG836262

Table 2. BLASTn analysis based on the DNA sequence of the *matK*.

Species Name	Query Cover (%)	E-Value	Identity (%)	Accession
<i>Calamus jenkinsianus</i>	100	0.0	99.53	ON248739.1
<i>Calamus tetradactylus</i>	100	0.0	99.29	NC_079772.1
<i>Calamus walker</i>	100	0.0	99.29	ON248637.1
<i>Calamus henryanus</i>	100	0.0	99.29	NC_079715.1
<i>Calamus aruensis</i>	100	0.0	99.29	AM114551.1
<i>Calamus castaneus</i>	100	0.0	99.06	JX903669.1
<i>Calamus caryotoides</i>	100	0.0	99.06	NC_020365.1
<i>Calamus viminalis</i>	100	0.0	98.94	JQ435566.1
<i>Pigafetta elata</i>	100	0.0	98.59	AM114549.1
<i>Metroxylon warburgii</i>	100	0.0	98.36	NC_029959.1

According to all phylogenetic tree analyses (Figure 3), the specimen species *C. angustifolius* formed a group with its fellow species, even though the specimens were taken from different areas. Phylogenetic analysis indicates that *C. angustifolius* shares a close genetic relationship with *C. aruensis*, *P. elata*, *C. viminalis*, and *C. castaneus*, suggesting a shared evolutionary lineage within the *Arecaceae* family. Genetic distance analysis results (Table 3) in data that the average genetic distance between individuals of the species being studied is 0,000. The lowest genetic gap between species studied with access from the Genbank is 0.007, with two different species types: *C. aruensis* and *P. elata*, whereas the highest genetical distance value is obtained in species *M. warburgii* with a value of 0.873.

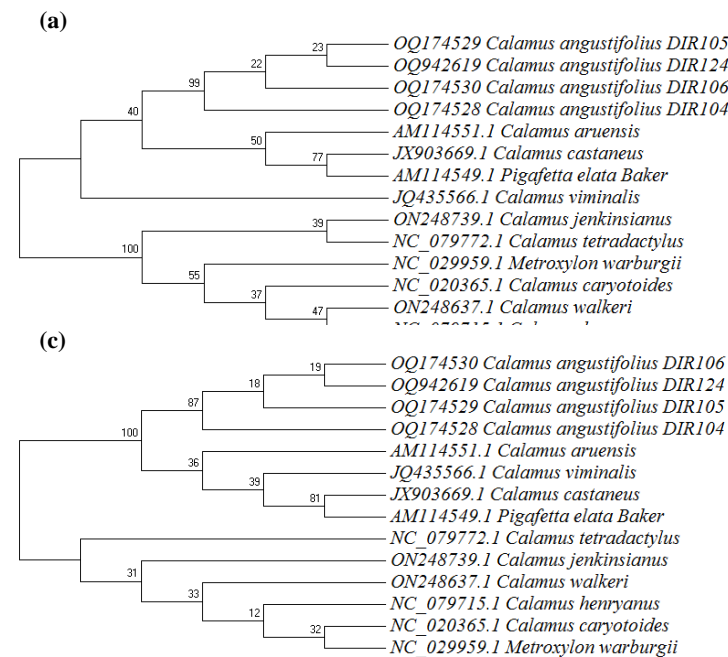


Figure 3. The Phylogenetics tree of *matK* sequences of all *Calamus angustifolius* accessions obtained from this study and related 10 accessions was inferred using the: (a) Maximum Likelihood method; (b) Maximum Parsimomial method; (c) Neighbour joining method. The bootstrap consensus tree was inferred from 1000 replicates.

Table 3. Genetic distance matrix based on the DNA sequence of the *matK* gene.

Species Name	1	2	3	4	5	6	7	8	9	10	11	12	13	14
1. <i>Calamus angustifolius</i> Teratak Buluh DIR104														
2. <i>Calamus angustifolius</i> Teratak Buluh DIR105	0.000													
3. <i>Calamus angustifolius</i> Teratak Buluh DIR106	0.000	0.000												
4. <i>Calamus angustifolius</i> Langgam DIR124	0.000	0.000	0.000											
5. <i>Calamus jenkinsianus</i>	0.860	0.860	0.860	0.860										
6. <i>Calamus tetradactylus</i>	0.856	0.856	0.856	0.856	0.005									
7. <i>Calamus walker</i>	0.856	0.856	0.856	0.856	0.005	0.002								
8. <i>Calamus henryanus</i>	0.856	0.856	0.856	0.856	0.005	0.002	0.000							
9. <i>Calamus aruensis</i>	0.007	0.007	0.007	0.007	0.856	0.853	0.852	0.852						
10. <i>Calamus castaneus</i>	0.010	0.010	0.010	0.010	0.870	0.866	0.865	0.865	0.005					
11. <i>Calamus caryotoides</i>	0.859	0.859	0.859	0.859	0.007	0.005	0.002	0.002	0.856	0.869				
12. <i>Calamus viminalis</i>	0.011	0.011	0.011	0.011	0.861	0.857	0.856	0.856	0.006	0.008	0.860			
13. <i>Pigafetta elata</i>	0.007	0.007	0.007	0.007	0.868	0.865	0.864	0.864	0.002	0.004	0.868	0.006		
14. <i>Metroxylon warburgii</i>	0.873	0.873	0.873	0.873	0.009	0.007	0.005	0.005	0.869	0.883	0.007	0.874	0.881	

An analysis of nucleotide variation in the *matK* gene showed that 542 nucleotides (59%) of the total aligned sequence were genetic variations. This number belongs to a large number and is a natural occurrence in the sequence of the *matK* gene. Three of these nucleotide variations are critical nucleotides that only the species *C. angustifolius* possesses. The critical nucleotide is the sequence number 46 (C on the water rattan and A on the other accessions), 439 (T on the water rattan, and G on other accessions), and 831 (T on the water rattan and A on the other accessions) (Table 4).

Table 4. Critical nucleotide in *matK* sequence of Water Rattan Palm (*Calamus angustifolius*) from Riau Province.

Accessions	Nucleotide number		
	46	439	831
<i>Calamus angustifolius</i> Teratak_Buluh_DIR104	C	T	T
<i>Calamus angustifolius</i> Teratak_Buluh_DIR105	.	.	.
<i>Calamus angustifolius</i> Teratak_Buluh_ DIR106	.	.	.
<i>Calamus angustifolius</i> Langgam_DIR124	.	.	.
<i>Calamus jenkinsianus</i>	A	G	A
<i>Calamus tetradactylus</i>	A	G	A
<i>Calamus walkeri</i>	A	G	A
<i>Calamus henryanus</i>	A	G	A
<i>Calamus aruensis</i>	A	C	C
<i>Calamus castaneus</i>	A	C	C
<i>Calamus caryotoides</i>	A	G	A
<i>Calamus viminalis</i>	A	C	C
<i>Pigafetta elata</i>	A	C	C
<i>Metroxylon warburgii</i>	A	G	A

The nucleotide substitution pattern was inferred using the maximum composite likelihood method, and the probability of substitution was estimated by Tamura *et al.* (Tamura *et al.*, 2004) model. For purines, the transition/transversion rate ratio is $k1 = 6.96$, while for pyrimidines it is $k2 = 7.556$. $R = 3.211$ represents the overall transition/transversion bias. $A = 32.88\%$, $T/U = 34.21\%$, $C = 16.62\%$, and $G = 16.29\%$ are the nucleotide frequencies (Table 5). The A+T frequency (67.09%) would be significantly higher than the C+G frequency (32.91%) if totaled. Nucleotides A have the highest frequencies compared to other nucleotides in codon 1 with a Frequency of 37.51%, whereas T in codons 2 and 3 with Frequencies of 39.30% and 29.83%, respectively. These evolutionary analyses were conducted in MEGA11 (Tamura *et al.*, 2021).

Table 5. Nucleotide composition in *matK* sequence

Sp.	T(U)	C	A	G	Total	T-1	C-1	A-1	G-1	Pos #1	T-2	C-2	A-2	G-2	Pos #2	T-3	C-3	A-3	G-3	Pos #3
1	38.21	17.69	29.13	14.98	848	37.46	16.61	32.51	13.43	283	44.52	12.72	28.27	14.49	283	32.62	23.76	26.60	17.02	282
2	38.21	17.69	29.13	14.98	848	37.46	16.61	32.51	13.43	283	44.52	12.72	28.27	14.49	283	32.62	23.76	26.60	17.02	282
3	38.21	17.69	29.13	14.98	848	37.46	16.61	32.51	13.43	283	44.52	12.72	28.27	14.49	283	32.62	23.76	26.60	17.02	282
4	38.21	17.69	29.13	14.98	848	37.46	16.61	32.51	13.43	283	44.52	12.72	28.27	14.49	283	32.62	23.76	26.60	17.02	282
5	28.89	15.21	37.97	17.92	848	27.92	14.84	44.52	12.72	283	32.16	13.78	37.10	16.96	283	26.60	17.02	32.27	24.11	282
6	29.25	14.98	37.85	17.92	848	28.27	14.84	44.17	12.72	283	32.86	13.07	37.10	16.96	283	26.60	17.02	32.27	24.11	282
7	29.01	15.09	37.85	18.04	848	28.27	14.84	44.17	12.72	283	32.51	13.43	37.10	16.96	283	26.24	17.02	32.27	24.47	282
8	29.01	15.09	37.85	18.04	848	28.27	14.84	44.17	12.72	283	32.51	13.43	37.10	16.96	283	26.24	17.02	32.27	24.47	282
9	37.97	17.81	29.13	15.09	848	37.10	16.96	32.51	13.43	283	44.52	12.37	28.27	14.84	283	32.27	24.11	26.60	17.02	282
10	37.85	18.04	29.01	15.09	848	37.10	16.96	32.51	13.43	283	44.17	12.72	27.92	15.19	283	32.27	24.47	26.60	16.67	282
11	29.01	14.98	37.97	18.04	848	28.27	14.84	44.17	12.72	283	32.51	13.43	37.10	16.96	283	26.24	16.67	32.62	24.47	282
12	38.09	17.69	29.25	14.98	848	37.46	16.96	32.16	13.43	283	44.52	12.01	28.98	14.49	283	32.27	24.11	26.60	17.02	282
13	37.70	17.80	29.39	15.11	854	36.84	16.84	32.98	13.33	285	43.86	12.63	29.12	14.39	285	32.39	23.94	26.06	17.61	284
14	29.27	15.22	37.59	17.92	854	29.12	14.39	43.86	12.63	285	32.63	13.68	36.84	16.84	285	26.06	17.61	32.04	24.30	284
Avg.	34.21	16.62	32.88	16.29	848.9	33.46	15.91	37.52	13.11	283.3	39.31	12.96	32.12	15.61	283.3	29.83	21.00	29.00	20.17	282.3

Note: (1-4) *C. angustifolius* (5) *C. jenkinsianus*, (6) *C. tetradactylus*, (7) *C. walkeri*, (8) *C. henryanus*, (9) *C. aruensis*, (10) *C. castaneus*, (11) *C. caryotoides*, (12) *C. viminalis*, (13) *Pigafetta elata*, and (14) *Metroxylon warburgii*.

3.3. Phylogenetic analysis for the *trnL-trnL-trnF* Intergenic Spacer

Using the universal primer from Taberlet *et al.* (1991), we obtained PCR products for *C. angustifolius trnL-trnL-trnF* IGS about 867 bp. The sequence was searched against a database using BLAST search, which shows all the top 10 BLASTn accessions had a similarity of 99% to *C. angustifolius trnL-trnL-trnF* IGS sequence (Table 6). The highest score is 99.77% similarity with multiple plant species *M. warburgii*, *C. caryotoides*, and also *C. hollrungii* that was not even found on the top 10 BLASTn accessions with *matK*. The difference in BLASTn results is quite striking between *matK* and *trnL-trnL-trnF* IGS.

Table 6. BLASTn analysis based on the DNA sequence of the *trnL-trnL-trnF* Intergenic Spacer.

Species Name	Query Cover (%)	E-Value	Identity (%)	Accession
<i>Metroxylon warburgii</i>	100	0.0	99.77	NC_029959.1
<i>Calamus caryotoides</i>	100	0.0	99.77	NC_020365.1
<i>Calamus hollrungii</i>	100	0.0	99.77	AJ241279.1
<i>Calamus jenkinsianus</i>	100	0.0	99.66	NC_067841.1
<i>Calamus tetradactylus</i>	100	0.0	99.65	NC_079772.1
<i>Salacca zalacca</i>	100	0.0	99.31	NC_063109.1
<i>Calamus henryanus</i>	100	0.0	99.20	NC_079715.1
<i>Eugeissona tristis</i>	100	0.0	99.42	AJ241278.1
<i>Salacca wallichiana</i>	100	0.0	99.09	ON248811.1
<i>Calamus walkeri</i>	100	0.0	99.09	ON248637.1

Looking at the phylogenetic tree result of this sequence (Figure 4), it appears that *C. angustifolius* still cannot be differentiated from most of the different species. Furthermore, the genetic distance analysis based on the *trnL-trnL-trnF* IGS sequences (Table 7) revealed that the average genetic distance among individuals of the studied species is 0,000. But, surprisingly, this value (0,000) is also obtained between species *C. angustifolius* with eight out of 10 BLASTn access tops. These species include *C. jenkinsianus*, *C. caryotoides*, *C. hollrungii*, *C. tetradactylus*, *S. zalacca*, *C. henryanus*, *S. wallichiana*, and *C. walkeri*. While the other two accessions (*M. warburgii* and *E. tristis*) are still detected, there are genetic distances that are supposed to exist between different species. Effective DNA barcoding depends on the marker's capacity to distinguish between closely related species, but this is hampered by the low variability of *trnL-trnL-trnF* IGS markers.

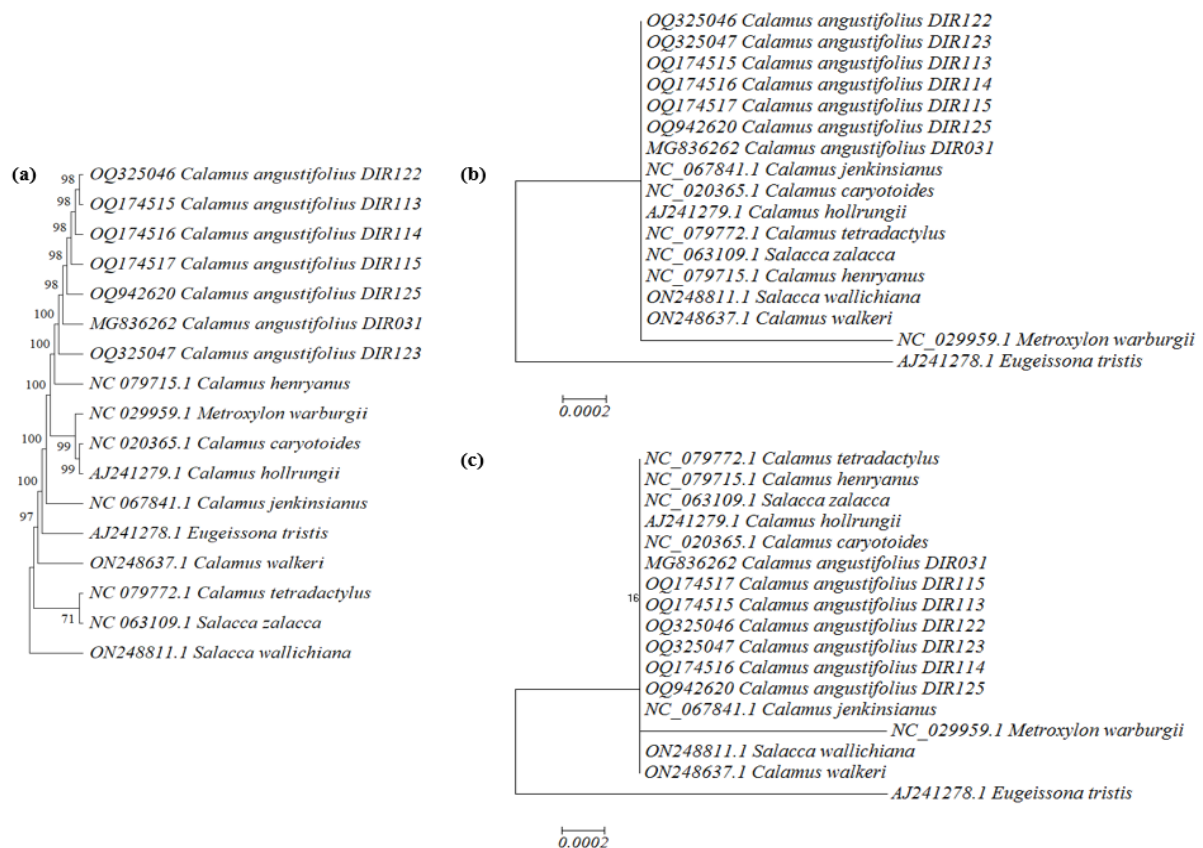


Figure 4. The Phylogenetics tree of *trnL-trnL-trnF* Intergenic Spacer sequences of all *Calamus angustifolius* accessions obtained from this study and related 10 accessions was inferred using the: (a) Maximum Parsimony method; (b) Maximum Likelihood method; (c) Neighbour joining method. The bootstrap consensus tree was inferred from 1000 replicates.

Table 7. Genetic distance matrix based on the DNA sequence of the *trnL-trnL-trnF Intergenic Spacer*.

Species Name	1	2	3	4	5	6	7	8	9	10	11	12	13	14	15	16	17
<i>Calamus angustifolius</i> Kualu DIR122																	
<i>Calamus angustifolius</i> Kualu DIR123	0.000																
<i>Calamus angustifolius</i> Teratak Buluh DIR1130.0000.000																	
<i>Calamus angustifolius</i> Teratak Buluh DIR1140.0000.0000.000																	
<i>Calamus angustifolius</i> Teratak Buluh DIR1150.0000.0000.0000.000																	
<i>Calamus angustifolius</i> Langgam DIR125	0.0000.0000.0000.0000.000																
<i>Calamus angustifolius</i> Langgam DIR031	0.0000.0000.0000.0000.0000.000																
<i>Calamus jenkinsianus</i>	0.0000.0000.0000.0000.0000.0000.000																
<i>Metroxylon warburgii</i>	0.0010.0010.0010.0010.0010.0010.0010.001																
<i>Calamus caryotoides</i>	0.0000.0000.0000.0000.0000.0000.0000.0000.001																
<i>Calamus hollrungii</i>	0.0000.0000.0000.0000.0000.0000.0000.0000.0010.000																
<i>Calamus tetradactylus</i>	0.0000.0000.0000.0000.0000.0000.0000.0000.0010.0000.000																
<i>Salacca zalacca</i>	0.0000.0000.0000.0000.0000.0000.0000.0000.0010.0000.0000.000																
<i>Calamus henryanus</i>	0.0000.0000.0000.0000.0000.0000.0000.0000.0010.0000.0000.0000.000																
<i>Eugeissona tristis</i>	0.0020.0020.0020.0020.0020.0020.0020.0020.0030.0020.0020.0020.0020.002																
<i>Salacca wallichiana</i>	0.0000.0000.0000.0000.0000.0000.0000.0000.0010.0000.0000.0000.0000.0000.002																
<i>Calamus walker</i>	0.0000.0000.0000.0000.0000.0000.0000.0000.0010.0000.0000.0000.0000.0000.0020.000																

The nucleotide variations analyzed were also only 26 variations, and could not find any critical nucleotides at all. The frequencies of the nucleotides are 35.07% for A, 31.00% for T/U, 17.95% for C, and 15.98% for G (Table 8). For purines, the transition/transversion rate ratio is $k1 = 0.947$, while for pyrimidines it is $k2 = 1.638$. $R = 0.577$ is the total bias for transition and transversion. Matches

matK, The A+T frequency (66.03%) would be significantly higher than the C+G frequency (33.95%) if totaled in *trnL-trnL-trnF IGS*. Nucleotides A have the highest frequencies compared to other nucleotides in codon 1, 2, and 3 with Frequencies of 35.18, 33.89%, and 36.09%, respectively. These results are also obtained in the same way as *matK*.

Table 8. Nucleotide composition in *trnL-trnL-trnF Intergenic Spacer* sequence.

Sp.	T(U)	C	A	G	Total	T-1	C-1	A-1	G-1	Pos #1	T-2	C-2	A-2	G-2	Pos #2	T-3	C-3	A-3	G-3	Pos #3
1	30.91	17.99	35.06	16.03	867	30.45	17.30	36.33	15.92	289	30.80	18.34	33.22	17.65	289	31.49	18.34	35.64	14.53	289
2	30.91	17.99	35.06	16.03	867	30.45	17.30	36.33	15.92	289	30.80	18.34	33.22	17.65	289	31.49	18.34	35.64	14.53	289
3	30.91	17.99	35.06	16.03	867	30.45	17.30	36.33	15.92	289	30.80	18.34	33.22	17.65	289	31.49	18.34	35.64	14.53	289
4	30.91	17.99	35.06	16.03	867	30.45	17.30	36.33	15.92	289	30.80	18.34	33.22	17.65	289	31.49	18.34	35.64	14.53	289
5	30.91	17.99	35.06	16.03	867	30.45	17.30	36.33	15.92	289	30.80	18.34	33.22	17.65	289	31.49	18.34	35.64	14.53	289
6	30.91	17.99	35.06	16.03	867	30.45	17.30	36.33	15.92	289	30.80	18.34	33.22	17.65	289	31.49	18.34	35.64	14.53	289
7	30.91	17.99	35.06	16.03	867	30.45	17.30	36.33	15.92	289	30.80	18.34	33.22	17.65	289	31.49	18.34	35.64	14.53	289
8	31.15	17.93	34.94	15.98	870	30.69	17.24	36.21	15.86	290	31.03	18.28	33.10	17.59	290	31.72	18.28	35.52	14.48	290
9	30.99	17.97	35.14	15.90	868	33.79	17.24	35.52	13.45	290	30.10	16.61	34.60	18.69	289	29.07	20.07	35.29	15.57	289
10	30.91	17.99	35.06	16.03	867	32.53	17.30	34.95	15.22	289	31.83	16.96	32.87	18.34	289	28.37	19.72	37.37	14.53	289
11	30.91	17.99	35.06	16.03	867	32.53	17.30	34.95	15.22	289	31.83	16.96	32.87	18.34	289	28.37	19.72	37.37	14.53	289
12	30.88	17.97	35.14	16.01	868	30.34	20.34	34.83	14.48	290	31.83	17.65	33.91	16.61	289	30.45	15.92	36.68	16.96	289
13	31.16	17.87	35.05	15.92	873	29.90	19.24	34.02	16.84	291	31.62	18.56	34.02	15.81	291	31.96	15.81	37.11	15.12	291
14	30.96	17.89	35.09	16.06	872	32.65	17.53	34.71	15.12	291	29.90	17.87	35.74	16.49	291	30.34	18.28	34.83	16.55	290
15	30.72	18.13	35.10	16.05	866	30.10	22.15	33.56	14.19	289	33.56	14.88	36.33	15.22	289	28.47	17.36	35.42	18.75	288
16	31.31	17.83	34.97	15.89	875	30.82	20.89	32.88	15.41	292	34.25	16.78	34.25	14.73	292	28.87	15.81	37.80	17.53	291
17	31.31	17.83	34.97	15.89	875	32.53	19.18	32.19	16.10	292	30.48	18.84	35.96	14.73	292	30.93	15.46	36.77	16.84	291
Avg.	30.98	17.96	35.06	16.00	869	31.12	18.21	35.18	15.49	290	31.30	17.75	33.90	17.06	290	30.53	17.93	36.10	15.45	289

4. Discussion

Phylogenetic tree analysis, supported by low genetic distance values based on the *matK* sequence, indicates that *C. angustifolius* from the Kampar River, Riau Province (Indonesia), is genetically very similar to *C. aruensis* and

P. elata. Furthermore, it also shows a close genetic relationship with *M. warburgii* and *C. jenkinsianus*. Investigating the molecular phylogenetic relationships among taxa can lead scientists to make new discoveries (Ha *et al.*, 2022).

If we compare based on their morphology, both *Calamus* species (*C. angustifolius* and *C. aruensis*) have

some very similar morphologies. The obvious difference is that the habitus of *C. aruensis* is a Robust, single- or rarely multi-stemmed rattan that can reach a height of 50 meters. The fruit is globose, cream-white in color, solitary, and has a short stalk. Broad in New Guinea, extending from the Bismarck Archipelago to the Raja Ampat Islands (Baker *et al.*, 2024). On the other hand, *P. elata* is a plant that is Large, straight, single-trunked, and belongs to the Araceae family (areca nuts). This plant also goes by the name "wanga" in Sulawesi. Mature plants have a trunk diameter of up to 40 cm and a maximum height of 50 meters. When the fruit is young, it is greenish, and as it ages it turns greenish-yellow. Other than its sour flavor, this fruit is rarely eaten and can result in yellowing teeth (Syamsiah *et al.*, 2018).

The close phylogenetic relationship indicates that these species might share genetic traits that contribute to their adaptability and resilience to environmental changes. This suggests that conservation strategies for these species can be coordinated. Conservation strategies can be optimized by managing the species within the same framework, which is especially important in regions where resources for conservation are limited. Understanding the genetic diversity and relationships among *Calamus* species can inform conservation strategies by identifying genetically distinct populations that may be prioritized for protection, thereby safeguarding valuable germplasm and promoting sustainable use. The sustainable management and harvesting of rattan, including *C. angustifolius*, are essential for forest conservation. Overharvesting or unsustainable practices can lead to habitat degradation, impacting biodiversity and ecosystem services.

The nucleotide composition in a DNA sequence has significant implications for the properties and functions of the genome of an organism. Some traits and genomic behavior are impacted by increased adenine (A) and thymine (T) compositions. There is an increased susceptibility to mutations because the A-T rich genome region tends to be less stable and more susceptible to denaturation under heat or chemical stress. These regions can denature more easily than G-C rich regions, which are more stable due to the stronger hydrogen bonds between guanine and cytosine pairs (Vinogradov and Anatskaya, 2017). While a higher A-T content is associated with certain genomic characteristics such as increased mutation rates, the implications for *C. angustifolius* require further investigation to determine any impact on its genome stability (Zhang *et al.*, 2022).

The nucleotide composition can affect the architecture of the entire genome. A-T rich areas, for instance, are frequently more pliable and flexible, which may have an impact on the chromatin's high-level structure. This may have an impact on procedures like chromatin remodeling and the nucleus's arrangement of the genome (Vergara and Gutierrez, 2017; Zagirova *et al.*, 2024). The A-T rich genome may also evolve differently from the G-C rich genomes due to variations in the rate of mutation and the pressure of selection. This has consequences for evolution. For instance, a rich area of A-T might experience a faster rate of mutation accumulation, leading to a higher level of genetic diversity there (Lynch *et al.*, 2016).

The transition rate ratios for purines and pyrimidines are k_1 and k_2 , respectively. In *matK* gene sequences, purins have a transition speed ratio of 6.96 ($k_1 = 6.96$).

This indicates that purines transversions (from A <-> G) are around 6.96 times less common than purines transitions. $k_2 = 7.556$: Pyrimidines transition rate ratios are 7.556. In other words, transitions involving pyrimidines are around 7.556 times less common than those using pyrimidines (C <-> T). The entire magnitude of the transition bias towards transversion is expressed as $R = 3.211$. This number indicates the frequency of transitions over the whole DNA sequence in comparison to transversions in general.

On the other hand, k_1 for purines in *trnL-trnL-trnF IGS* region has a ratio of transitions to transversions is 0.947. This suggests that transitions are less frequent than transversions among purines. While k_2 for pyrimidines has a ratio of transitions to transversions is 1.638. This indicates that transitions are more frequent than transversions among pyrimidines. The value of overall transition/transversion bias is $R = 0.577$. The transition/transversion rate ratios (k_1 and k_2) indicate the frequency of nucleotide substitutions, with higher values suggesting a bias towards transitions (substitutions between purines or between pyrimidines) over transversions (substitutions between a purine and a pyrimidine). The overall bias (R) supports this preference, which is common in molecular evolution due to the less disruptive nature of transitions. A value less than 1 indicates a higher frequency of transversions than transitions in the entire sequence.

Higher nucleotide diversity in the *matK* region made it possible to distinguish across species more clearly and strengthened its usefulness as a marker in genetic research. In this study, the *trnL-trnL-trnF IGS* region demonstrated limited variability among *Calamus* species, restricting its effectiveness for species differentiation within this genus. This statement is supported by the genetic distance result generated by the *trnL-trnL-trnF IGS* sequence in *C. angustifolius* with the top 10 accessions of BLASTn not being able to discriminate or differentiate between the species. The species that are taxonomically different such as *S. zalacca* and *S. wallichiana*, cannot be distinguished (the value remains 0.000), let alone to species that belong to his genus. In addition, phylogenetic analysis continues to classify *C. angustifolius* among distantly related species. Individuals within the same species will be grouped into a single cluster on the phylogenetic tree, distinct from individuals belonging to other species. So, we decided that the *trnL-trnL-trnF IGS* sequence has no power to be used as a DNA barcode for the species *C. angustifolius*. Molecular markers such as single nucleotide polymorphisms (SNPs) and internal transcribed spacers (*ITS*) are increasingly used in plant identification because it has a greater resolution for genetic diversity studies (Schwartz *et al.*, 2007) and offers promising avenues for future research on *Calamus* species.

Since purines and pyrimidines generally result in more persistent and subtle modifications to DNA structure, their high transition/transversion ratios suggest that transitions happen more frequently. Nucleotide transitions are repeatedly preferred over transversions in molecular evolution. The role of selection is often cited in explanations for this pattern of amino acid modifications because transitions have more conservative effects on proteins (Stoltzfus and Norris, 2016). Evolution and mutation processes frequently reveal a greater frequency of

transitions than transversions. Numerous reasons might be blamed for this bias, including chemical stability, DNA repair mechanisms, and natural selection's tendency to preserve the genome's stability (Lyons and Luring, 2017). In summary, the statement describes an analysis of nucleotide variations and frequencies, highlighting that transitions and transversions have different rates depending on the nucleotide type, with an overall bias favoring transversions.

5. Conclusions

This study validated that the barcoding DNA technique using *matK* can better identify *Calamus* plant species, especially *C. angustifolius*. These findings underscore the value of the *matK* gene in genetic and taxonomic studies of *Calamus*, providing a foundation for future research aimed at conservation and sustainable management of water rattan populations. The *trnL-trnL-trnF intergenic spacer*, however, was less effective in this role. In the future, we also suggest the use of *matK* for analysis to solve taxonomic problems in the genus *Calamus*.

Acknowledgements

This research was fully sponsored by a grant from DIPA Universitas Riau year 2023 under "Unggulan Universitas Riau" with contract number 8345/UN19.5.1.3/AL.04/2023. Thanks to LPPM of Universitas Riau.

References

Al-Rawashdeh IM. 2011. Molecular taxonomy among *Mentha spicata*, *Mentha longifolia* and *Ziziphora tenuior* populations using the RAPD Technique. *Jordan J Biol Sci.*, **4(2)**: 63–70.

Amandita FY, Rembold K, Vornam B, Rahayu S, Siregar IZ, Kreft H and Finkeldey R. 2019. DNA barcoding of flowering plants in Sumatra, Indonesia. *Ecol Evol.*, **9(4)**: 1858–1868.

Antil S, Abraham JS, Sripoorna S, Maurya S, Dagar J, Makhija S, Bhagat P, Gupta R, Sood U and Toteja R. 2023. DNA barcoding, an effective tool for species identification: a review. *Mol Biol Rep.*, **50(1)**: 761–775.

Awomukwu DA, Nyananyo BL, Uka CJ, Spies P and Sizani BL. 2015. DNA barcoding, identification and validation of the genus *Phyllanthus* in Nigeria using plastid *rbcL* and *matK* genetic markers. *GJSFR-G.*, **15(1)**.

Ayu DF. 2018. **Ensiklopedia Produk Pangan Indonesia**, third ed. PT. Penerbit IPB Press, Bogor.

Baker WJ. 2015. A revised delimitation of the rattan genus *Calamus* (Arecaceae). *Phytotaxa.*, **197(2)**: 139–152.

Baker WJ, Barford AS, Cámara-Leret R, Dowe JL, Heatubun CD, Petoe P, Turner JH, Zona S, Dransfield J and Smith LT. 2024. **The Palms of New Guinea**. Royal Botanic Gardens, Kew, United Kingdom.

Baldwin BG, Sanderson MJ, Porter JM, Wojciechowski MF, Campbell CS and Donoghue ML. (1995). The ITS region of nuclear ribosomal DNA: A valuable source of evidence on angiosperm phylogeny. *Ann Missouri Bot Gard.*, **82(2)**: 247–277.

Borsch T and Quandt D. 2009. Mutational dynamics and phylogenetic utility of noncoding chloroplast DNA. *Plant Syst Evol.*, **282(3–4)**: 169–199.

CBOL Plant Working Group. 2009. A DNA barcode for land plants. *Proc Natl Acad Sci USA.*, **106**: 12794–12797.

Chac LD and Thinh BB. 2023. Species identification through dna barcoding and its applications: A review. *Biol Bull.*, **50(6)**: 1143–1156.

Davey JW and Blaxter ML. 2010. RADSeq: Next-generation population genetics. *Brief Funct Genomics.*, **9(5–6)**: 416–423.

Felsenstein J. 1985. Confidence limits on phylogenies: an approach using the bootstrap. *Evolution.*, **39(4)**: 783–791.

Ha DC, Cao PB, Nguyen VD and Le CT. 2022. Molecular phylogeny and deep origins of the hybrid mokara dear heart (Orchidaceae). *Jordan J Biol Sci.*, **15(5)**: 805–811.

Hall TA. 1999. BioEdit: a user-friendly biological sequence alignment editor and analysis program for windows 95/98/NT. *Nucleic Acids.*, **41**: 95–98.

Heckenhauer J, Barfuss MHJ and Samuel R. 2016. Universal multiplexable *matK* primers for DNA barcoding of angiosperms. *Appl Plant Sci.*, **4(6)**.

Herman, Al-Khairi H, Wansyah AR, Asmania, Utami RI, Anzaelina DN, Oktaviano Z, Lestari W, Adiwirman, and Roslim DI. 2023. The Ability of *matK* and *trnL-trnL-trnF* intergenic spacer to discern certain species accessions of the Families Solanaceae and Fabaceae. *SABRAO J Breed Genet.*, **55(1)**: 97–106.

Ho VT, Tran TKP, Vu TTT and Widiarsih S. 2021. Comparison of *matK* and *rbcL* DNA barcodes for genetic classification of jewel orchid accessions in Vietnam. *J Genet Eng Biotechnol.*, **19(1)**.

Kaliky F. 2018. Identification of the types of rattan in the home industry in Waitatiri Village, Salahutu District, Central Maluku Regency. *Jurnal Agrohut.*, **9(1)**.

Kar P and Goyal AK. 2015. Maturase K gene in plant DNA barcoding and phylogenetics. In: Ali MA, Gabor G, Al-Hemaid F (Eds.). **Plant DNA Barcoding and Phylogenetics**. Lambert Academic Publishing, Germany. pp. 79–90.

Kurian A, Dev SA, Sreekumar VB and Muralidharan EM. 2020. The low copy nuclear region, RPB2 as a novel DNA barcode region for species identification in the rattan genus *Calamus* (Arecaceae). *Physiol Mol Biol Plants.*, **26(9)**: 1875–1887.

Lynch M, Ackerman MS, Gout J, Long H, Sung W, Thomas WK and Foster PL. 2016. Genetic drift, selection and the evolution of the mutation rate. *Nat Rev Genet.*, **17**: 704–714.

Lyons DM and Luring AS. 2017. Evidence for the selective basis of transition-to-transversion substitution bias in two RNA viruses. *Mol Biol Evol.*, **34(12)**: 3205–3215.

Maddison WP and Maddison DR. 2023. **Mesquite: a modular system for evolutionary analysis**. Version 3.81. <http://www.mesquiteproject.org>.

Mir RA, Bhat KA, Rashid G, Ebinezer LB, Masi A, Rakwal R, Shah AA and Zargar SM. 2021. DNA barcoding: a way forward to obtain deep insights about the realistic diversity of living organisms. *Nucleus.*, **64(2)**: 157–165.

Mustafa KM, Ewadh MJ, Al-Shuhaib MBS and Hasan HG. 2018. The in silico prediction of the chloroplast maturase K gene polymorphism in several barley varieties. *Agriculture (Pol'nohospodarstvo).*, **64(1)**: 3–16.

Myers R. 2015. What the Indonesian rattan export ban means for domestic and international markets, forests, and the livelihoods of rattan collectors. *For Policy Econ.*, **50**: 210–219.

Odah MAA. 2023. Unlocking the genetic code: Exploring the potential of DNA barcoding for biodiversity assessment. *AIMS Mol Sci.*, **10(4)**: 263–294.

Roslim DI. 2017. Identification of pandan plant (*Benstonea* sp.) from Riau, Indonesia using three DNA barcodes. *SABRAO J Breed Genet.*, **49(4)**: 346–360.

- Roslim DI, Khumairoh S and Herman. 2016. Confirmation of tuntun angin (*Elaeocarpus floribundus*) taxonomic status using matK and ITS sequences. *Biosaintifika.*, **8(3)**: 393.
- Schwartz MK, Luikart G and Waples RS. 2007. Genetic monitoring as a promising tool for conservation and management. *Trends Ecol Evol.*, **22(1)**: 25-33.
- Shaw J, Lickey EB, Schilling EE and Small RL. 2007. Comparison of whole chloroplast genome sequences to choose noncoding regions for phylogenetic studies in angiosperms: The Tortoise and the hare III. *Am J Bot.*, **94(3)**: 275-288.
- Siebert, S. F. (2005). The abundance and distribution of rattan over an elevation gradient in Sulawesi, Indonesia. *For Ecol Manage.*, **210(1-3)**, 143-158.
- Stoltzfus A and Norris RW. 2016. On the causes of evolutionary transition:transversion bias. *Mol Biol Evol.*, **33(3)**: 595-602.
- Suleiman MS, Wasonga VO, Mbau JS, Suleiman A and Elhadi YA. 2017. Non-timber forest products and their contribution to households income around Falgore Game Reserve in Kano, Nigeria. *Ecol Process.*, **6(1)**.
- Syamsiah, Hala Y, Hiola SF and Azis K. 2018. Local knowledge of wanga (*Pigafetta elata*) as materials of traditional house at South Sulawesi, Indonesia. In *AIP Conference Proceedings*, Vol. 2030, American Institute of Physics Inc.
- Taberlet P, Gielly L, Pautou G and Bouvet J. 1991. Universal primers for amplification of three non-coding regions of chloroplast DNA. *Plant Mol Biol.*, **17(5)**: 1105-1109.
- Tamura K, Nei M and Kumar S. 2004. Prospects for inferring very large phylogenies by using the neighbor-joining method. *Proc Natl Acad Sci USA.*, **101(30)**: 11030-11035.
- Tamura K, Stecher G and Kumar S. 2021. MEGA11: Molecular Evolutionary Genetics Analysis Version 11. *Mol Biol Evol.*, **38(7)**: 3022-3027.
- Tanaka S and Ito M. 2020. DNA barcoding for identification of agarwood source species using trnL-trnF and matK DNA sequences. *J Nat Med.*, **74(1)**: 42-50.
- Thompson JD, Higgins DG and Gibson TJ. 1994. CLUSTAL W: improving the sensitivity of progressive multiple sequence alignment through sequence weighting, position-specific gap penalties and weight matrix choice. *Nucleic Acids Res.*, **22**: 4673-4680.
- Vergara Z and Gutierrez C. 2017. Emerging roles of chromatin in the maintenance of genome organization and function in plants. *Genome Biol.*, **18(1)**.
- Vinogradov AE and Anatskaya OV. 2017. DNA helix: the importance of being AT-rich. *Mamm Genome.*, **28(9-10)**: 455-464.
- Yao G, Zhang YQ, Barrett C, Xue B, Bellot S, Baker WJ and Ge XJ. 2023. A plastid phylogenomic framework for the palm family (Arecaceae). *BMC Biol.*, **21(1)**.
- Zagirova D, Kononkova A, Vaulin N and Khrameeva E. 2024. From compartments to loops: understanding the unique chromatin organization in neuronal cells. *Epigenetics Chromatin.*, **17(1)**.
- Zhang Y, Wu L, Wang Z, Wang J, Roychoudhury S, Tomasik B, Wu G, Wang G, Rao X and Zhou R. 2022. Replication stress: A review of novel targets to enhance radiosensitivity-from bench to clinic. *Front Oncol.*, **12**.